Relaxation phenomena in AOT-water-decane critical and dense microemulsions

L. Letamendia[a,*], E. Pru-Lestret[a], P. Panizza[a], J. Rouch[a], F. Sciortino[b], P. Tartaglia[b], C. Hashimoto[c], H. Ushiki[c], D. Risso[d]

[a]*Centre de Physique Moléculaire Optique et Hertzienne, UMR 5798, Université Bordeaux I, 351 Cours de la Libération 33405 Talence, France*
[b]*Dipartimento di Fisica, Università di Roma La Sapienza, Piazzale Aldo Moro 2, Rome, Italy*
[c]*Laboratory of Transport and Transformation in Bio-systems, Department of Biomechanics and Intelligent Systems, Tokyo University of Agriculture and Technology, 3-5-8 Saiwai-Cho, Fuchu-shi, Tokyo 183, Japan*
[d]*Departamento de Fisica, Universidad del Bio-Bio, Av. Collao, 1202, Concepcion, Chile*

Received 28 March 2001

Abstract

We report on extensive measurements of the low and high frequencies sound velocity and sound absorption in AOT-water-decane microemulsions deduced from ultrasonic and, for the first time as far as the absorption is concerned, from Brillouin scattering experiments. New experimental results on dielectric relaxation are also reported. Our results, which include data taken for critical as well as dense microemulsions, show new interesting relaxation phenomena. The relaxation frequencies deduced from very high frequency acoustical measurements are in good agreement with new high frequency dielectric relaxation measurements. We show that along the critical isochore, sound dispersion, relaxation frequency, and static dielectric permittivity can be accurately fitted to power laws. The absolute values of the new exponents we derived from experimental data are nearly equal, and they are very close to $\beta = 0.33$ characterising the shape of the coexistence curve. The exponent characterising the infinite frequency permittivity is very close to 0.04 relevant to the diverging shear viscosity. For dense microemulsions, two well defined relaxation domains have been identified and the temperature variations of the sound absorption and the zero frequency dielectric permittivity bear striking similarities. We also show that the relaxation frequency of the slow relaxation process is almost independent of temperature and volume fraction and so cannot be attributed to percolation phenomena, whereas it can more likely be attributed to an intrinsic relaxation process probably connected to membrane fluctuations. © 2001 Elsevier Science B.V. All rights reserved.

PACS: 78.35.+c; 77.22.Gm; 66.20.+d; 64.60.Fr

* Corresponding author. Tel.: +33-556-84-62-07; fax: +33-556-84-69-70.
E-mail address: letame@cribx1.u-bordeaux.fr (L. Letamendia).

1. Introduction

It has been shown by Schulman [1] in the 40s that a mixture of oil, water, surfactant and eventually co-surfactant (long chain alcohol) can form a transparent homogeneous and thermodynamically stable systems known as microemulsions. The microemulsions can be made of water droplets coated by a surfactant monolayer floating in a bath of oil, the diameter of the droplets being typically 150 Å (inverse or water-in-oil microemulsion) or of direct oil-in-water microemulsion. It was realised in the mid-70s that the phase diagram of these systems was extremely rich. Upon varying the physical parameters characterising the system like the chemical nature of the surfactant (ionic or non-ionic) and of the oil, the volume fraction Φ of the dispersed phase, the temperature, etc., it has been possible to observe different type of phases with various morphological structure like droplet phases, bicontinuous phases, sponge phases, lamellar phases, liquid crystal phases, etc. to evidence phase traditions like cloud point curves and percolation phenomena.

Among the various types of microemulsions, one of the most interesting is the ternary system water-decane-AOT (di-2 ethylhexyl sodium sulphosuccinate), the AOT molecule being an ionic surfactant having a polar head and two hydrocarbon bulky tails. The surfactant film made of AOT possesses a spontaneous curvature directed toward water due to hydrophilicity–lipophilicity imbalance of the AOT. At room temperature, in the Gibbs phase diagram one observes a large one-phase region (L_2 region) extending from the decane corner into the middle of the Gibbs triangle. The dilution of the microemulsion can be achieved by adding decane to the solution. The phase diagram of this system at a value of the molar ratio X of [Water]/[AOT] equal to 40.8 is given in Fig. 1 of Ref. [2]. It shows a cloud point curve with a lower critical point located close to $T_C = 40^\circ C$ and $\Phi_C = 10\%$. It has been shown by neutron scattering that the water droplets (in this case water-in-oil) are identical below and above the critical temperature in the disordered and ordered system, respectively. This demonstrates that the critical microemulsion can be treated much like a binary system, the order parameter of the second order phase transition being the volume fraction Φ of the dispersed phase. At high volume fractions, $\Phi > 42\%$, the system displays other types of phases such as bicontinuous phases, sponge L_3 phases, L_α lamellar phases and eventually, at high temperature, a direct oil-in-water microemulsion phase (Fig. 1 of Ref. [2]).

The low frequency electrical conductivity σ of the microemulsion system has been measured as a function of both the volume fraction and the temperature [3–7]. A huge increase of the conductivity by about three orders of magnitude associated to a percolation phenomenon is observed. The latter is mediated by the hopping of the charges carried by the Na^+ counter-ions on a transient fractal network made by the droplets interacting via an attractive pair potential. For each volume fraction, the position of the percolation point is defined by the inflexion point in the plot of σ vs. T. The electrical conductivity percolation locus constructed using this procedure, cross over the phase diagram (Fig. 1 of Ref. [2]). It starts in the immediate vicinity of the critical point at high temperature and low volume fraction, down to low temperature and high volume fraction.

Microemulsions used as model systems have been studied by many different experimental techniques such as quasi-elastic light scattering, neutron scattering, small-angle X-ray scattering, ultrasonic methods, dielectric spectroscopy, molecular dynamic simulations, etc. As far as the quasi-elastic light scattering is concerned, light beating spectroscopy has been extensively used for the study of the concentration fluctuations which are reflected in the Rayleigh or non-shifted central line. Measurements of its line width lead to the mass diffusion coefficient of the droplets which shows an anomalous behaviour close to the consolute liquid–liquid critical point [8]. On the other hand, very few measurements have been reported on the Brillouin lines [9–11], the frequency shifted components of the polarised scattered light of a fluid. Brillouin lines are physically connected to the diffraction of the light on the thermal sound waves (pressure fluctuations) propagating at the speed of sound in the mixture. A Brillouin scattering experiment allows us to measure the sound velocity and the sound absorption at very high frequencies typically in the GHz range. Ultrasonic techniques allow us to perform nearly similar measurements but in the MHz range and even in the kHz domain. Using this techniques, extensive experiments on AOT based systems have been previously performed by Ye et al. [10], Zana et al. [12], Cametti et al. [13], Harada and Tabuchi [14]. Therefore, by combining these two experimental methods it is possible to deduce the sound dispersion properties in a very large frequency range. On the other hand, from time domain reflectometry experiments [15], one can sample high frequency dielectric properties of the system.

In this paper, we will first summarise some results of the hydrodynamic theory of thermal fluctuations for binary fluids, and then on the theory of mode coupling. In the next section, we will give some details on the Brillouin scattering experimental set-up and of time domain reflectometry which are not standard techniques. Next, we shall describe and discuss the new experimental results we obtained both at very high (Brillouin) and low (ultrasounds) frequencies. We will compare these results with those we inferred from dielectric relaxation spectroscopy both in time and frequency domains. All these experiments have been conducted as a function of both temperature and volume fraction. As we shall see in this paper, our new extensive set of experiments leads, for instance, to the observation of new scaling behaviours in temperature of some physical properties like sound dispersion, dielectric permittivities, relaxation frequencies and some unexpected effects like the complete similar behaviour between the high frequency sound absorption and the electrical conductivity for dense microemulsion when crossing the percolation threshold.

2. Theoretical background

2.1. Hydrodynamic model of a binary fluid

It has been shown [8] that microemulsion can be treated much like a binary fluid. In a Rayleigh–Brillouin scattering experiment one measures the dynamic structure factor

$S(q, \omega)$ which is proportional to the Fourier transform of the space and time dependent correlation function of the dielectric constant fluctuations. In terms of statistically independent variables, these fluctuations can in turn be written as a function of the local velocity, pressure, temperature and a linear combination of pressure and temperature. The details of the calculation are given by Berne and Pecora [16] and will not be reproduced here. The eigen frequencies of the system are the complex frequencies for which the determinant of the 4×4 hydrodynamic matrix is zero. In the case of a binary mixture one obtains four roots. Two roots s_1 and s_2 are real and correspond to the unshifted Rayleigh line. They are approximately given by

$$s_{1,2} = -\frac{q^2}{2} \left\{ \left(\frac{\lambda}{\rho_0 c_p} + \boldsymbol{D} \right) \pm \left[\left(\frac{\lambda}{\rho_0 c_p} + \boldsymbol{D} \right)^2 - 4\frac{\lambda D}{\rho_0 c_p} \right]^{1/2} \right\}, \tag{1}$$

where

$$\boldsymbol{D} = D \left[1 + \frac{k_T^2}{c_p T} \left(\frac{\partial \mu}{\partial c} \right)_{\rho, T} \right].$$

In the above equations, λ is the thermal conductivity, ρ_0 the mass density, c_p the specific heat at constant pressure, D the mass diffusion coefficient, μ the chemical potential and k_T the thermal diffusion coefficient. q is the wave vector of the thermal fluctuation selected by the experimental set-up: $q = (4\pi n/1)\sin\theta/2$, where n, 1, and θ are, respectively, the refractive index of the sample, the laser wavelength in vacuum and the scattering angle.

The two complex roots s_3 and s_4 which are responsible for the shift in Brillouin lines, are given by $s_{3,4} = -\Gamma_B \pm i\Omega_B$, where the frequency shift is $\Omega_B \approx qu$, u being the adiabatic "thermodynamic" sound velocity. Γ_B, the Brillouin line half width, represents the damping of the sound wave. The latter is given by

$$\Gamma_B = \frac{q^2}{2\rho_0} \left[\frac{4}{3}\eta_s + \eta_B + \left(\frac{c_p - c_v}{c_v} \right) \frac{\lambda}{c_p} + \rho_0^4 D u^2 \left(\frac{\partial \mu}{\partial c} \right)_{\rho, T} \left(\frac{k_p}{\rho_0} + \frac{k_T \alpha_T}{\rho_0 c_p} \right)^2 \right]. \tag{2}$$

In formula (2), c_v is the specific heat at constant volume, α_T is the thermal expansion coefficient, η_s and η_B are, respectively, the shear and the bulk (compressional) viscosities;

$$k_T = \frac{T_0}{D\rho_0} \left[a \left(\frac{\partial \mu}{\partial T} \right)_{c, P} + b \right]$$

is a transport coefficient. In this relation, T_0 is the equilibrium temperature and a and b are singular Onsager's coefficients. On the other hand, k_P, the barodiffusion coefficient only depends on the thermodynamical properties of the mixture. It is given by $k_P = -\frac{P_0}{\rho_0^2} \frac{(\partial \rho/\partial c)_{P,T}}{(\partial \mu/\partial c)_{P,T}}$, where P_0 is the equilibrium pressure.

Accounting for the numerical values for the scattering wave vector q of the order of 1.5×10^7 m^{-1} and the sound velocity u typically 1000 ms^{-1}, the two complex roots

are connected to very high frequency propagative sound modes, typically of the order 5 GHz. So, the frequency shift $\pm\Omega_B$ is in fact proportional to the hyper sound velocity u_∞, which is slightly larger than the ultrasonic velocity u:

$$u_\infty \approx u\left(1 + \frac{\Gamma_B^2}{2\Omega_B^2}\right) . \tag{3}$$

This comes from the fact that in Brillouin scattering experiments the scattering wave vector q is fixed and real, whereas in ultrasound experiments, it is the frequency ω which is imposed upon.

Once the eigen frequencies of the hydrodynamic matrix are known, it is easy to calculate the Rayleigh–Brillouin spectrum and show that it is constituted of two unshifted Lorentzian lines of half width $-s_1$ and $-s_2$ and two shifted Brillouin lines constituted by a Lorentzian and an anti-symmetric Lorentzian both centered on frequency $\pm\Omega_B$ and of half width Γ_B.

In the case of ultrasonic measurements, one induces a pressure wave in the mixture located in between two PZT transducers. By changing the spacing between the two transducers and measuring the positions and the amplitudes of the pressure maxima due to the pressure stationary waves, one is able to deduce the sound velocity u and the sound absorption coefficient α/f^2 at frequency $f = \omega/2\pi$ directly. The latter is directly proportional to the Brillouin line half width Γ_B and is given by

$$\frac{\alpha}{f^2} = \frac{4\pi^2\Gamma_B}{q^2 u^3} . \tag{4}$$

It is interesting to compare this value of the sound absorption to the so-called classical absorption $(\alpha/f^2)_{\text{class}}$ merely due to the static shear viscosity:

$$\left(\frac{\alpha}{f^2}\right)_{\text{class}} = \frac{8\pi^2}{3\rho_0 u^3}\eta_s . \tag{5}$$

2.2. Sound absorption and sound velocity near a critical point

2.2.1. Hydrodynamic regime

Close to a consolute point of a binary mixture, some thermodynamic and transport coefficients like D, $\frac{\partial\mu}{\partial c}$, k_p, k_T, η_s are anomalous. The diffusion coefficient D varies like τ^v, where τ is the reduced temperature $\tau = (T_C - T)/T_C$, and $v = 0.62$ is the critical exponent characterising the long range correlation length; $\partial\mu/\partial c$ varies like τ^γ, where $\gamma = 2v = 1.24$. Similarly, the barodiffusion coefficient k_P diverges like $\tau^{-\gamma}$ [17], and as shown by Giglio and Vedramini [18,19], the thermal–diffusion coefficient k_T scales like $\tau^{-\gamma}$. So in the vicinity of a critical point, the two central modes are decoupled and the Rayleigh central line is constituted by a pure mass diffusion mode showing a critical slowing down of half width $\Gamma_1 = D_{q^2}$, and a pure non-singular entropy (thermal) mode of half width $\Gamma_2 = \lambda q^2/\rho_0 c_p$. Typically, in this case, Γ_1 is of the order of few kHz, whereas Γ_2 is nearly 20 MHz, as in a normal liquid.

It is more difficult to discuss the respective contributions of the various terms involved in the widths of the Brillouin line. As shown by Mallamace et al. [11,20],

and by Berg and Moldover [21], the shear viscosity of the critical microemulsion deduced from experiments diverges like $\tau^{-0.04}$. Furthermore, according to the results given above, the term

$$D \left(\frac{\partial \mu}{\partial c} \right)_{\rho, T} \left(\frac{k_\mathrm{p}}{P_0} + \frac{k_\mathrm{T} \alpha_\mathrm{T}}{\rho_0 c_\mathrm{p}} \right)^2 ,$$

which appears in Eq. (2) should diverge like τ^{-v}, but little is known about the value of this term. However, very recent experiments by Delville et al. [22] on phase transitions induced by lasers have first confirmed the scaling form of k_T given above and have also provided the amplitude $k_\mathrm{T}^0 \approx 3$ of this coefficient in the case of a quaternary microemulsion made of water, dodecane, sodium dodecyl sulphate and pentanol. Therefore, in the hydrodynamic regime, one would expect a singular behaviour of the sound absorption close to the critical temperature T_c. On the other hand, since the adiabatic compressibility is assumed to behave in a normal way in a critical binary fluid, no singularity is a priori expected on the low frequency sound velocity.

2.2.2. Mode coupling theory of the critical-point singularity

The problem of sound propagation in the immediate vicinity of a liquid–gas critical point or near a consolute point in a binary liquid in the non-hydrodynamic regime, has been tackled by different authors. Besides the classical sound absorption calculated in the previous section, the theoretical results obtained by these authors predict an extra critical absorption and an anomaly of the sound velocity. A mode-coupling theory of sound propagation has been developed by Kawasaki [23] for a pure fluid, and then by D'Arrigo et al. [24,25] and Mistura [26] for a binary mixture. Later, more accurate expressions of the sound absorption and dispersion have been derived by Ferrell and Bhattacharjee [27] from their dynamic scaling theory of a critical binary fluid.

Close to a consolute point, the critical sound dispersion and attenuation at frequency ω can be written as a function of a reduced scaling variable $\omega^* = \omega/\omega_\mathrm{D}$, where ω_D, the Debye frequency is: $\omega_\mathrm{D} = 2D\xi^{-2}$. In this model, the diffusion coefficient D close to the critical point is given by its Stokes–Einstein expression: $D = k_\mathrm{B} T_\mathrm{c}/6\pi\eta\xi$. Assuming that the correlation length ξ scales like $\xi = \xi_0 \tau^{-v}$, where ξ_0 is the short range correlation length, leads to a Debye frequency varying like $\omega_\mathrm{D} = \omega_0 \tau^{3v}$, i.e., approaches zero rapidly upon approaching T_c.

In Kawasaki's theory [23], it is assumed that a complex longitudinal viscosity is relaxing, whereas in D'Arrigo et al. [24,25] and Mistura [26] and in Ferrell and Bhattacharjee [27] models, the relaxing quantity is the complex heat capacity. In both models, the sound attenuation and the velocity dispersion are given by the product of the same complex scaling function $I(\omega^*)$ of the scaling variable ω^* by a non-universal amplitude. For the sake of simplicity, we give here the Garland and Sanchez [28,29] expressions derived from Ferrell and Bhattacharjee [27].

$$\frac{\alpha}{f^2} = \frac{1}{2} u\omega A(\tau) \mathfrak{I}_\mathrm{m}[I(\omega^*)] , \tag{6}$$

where $\mathfrak{I}_m[I(\omega^*)]$ is the imaginary part of an integral involving Kawasaki's dynamical scaling function of the scaling variable $x = q\xi$ and the amplitude $A(\tau)$ is a weakly diverging function of temperature with the index $\hat{\alpha} = 0.11$. At constant temperature, this model leads to a sound absorption coefficient scaling in frequency like $\omega^{-0.96}$. Within the same approximations, the sound velocity $\tilde{u}(\omega)$ at frequency ω is given by

$$\tilde{u}(\omega) = u_c + \frac{g^2 u_c^3}{2T_c}[c_B + \mathfrak{R}_e(\tilde{c}_p(\omega))]^{-1}, \tag{7}$$

where $\tilde{c}_p(\omega)$ is the complex frequency-dependent specific heat which can be expressed by the real part of $I(\omega^*)$, c_B the background specific heat, u_c the critical limit value of the sound velocity at T_c and g a coupling constant. These models account well for both the anomalous absorption and dispersion of the sound velocity in critical molecular binary mixtures cyclohexane + nitroethane and 3-methyl pentane + nitroethane observed by Garland and Sanchez [28,29]. In particular, they explain why the sound velocity anomaly which is expected to be very weak, is so difficult to observe experimentally.

Weak anomalous behaviours have also been observed for the mass density ρ_0, the refractive index n and the static dielectric constant ε and it has been shown by Sengers et al. [30] that all these quantities are finite at the critical point.

If the electrical behaviour of percolating mixtures is now well understood, then as far as we know no firm theory exists to explain the sound propagation in these systems. However, de Gennes [31] has shown that the exponents characterising the elasticity properties of the systems are the same as those relative to electrical conductivity. These arguments have been supported by Ye et al. [10] findings, showing that the additional elastic modulus scales as a function of the volume fraction, with an exponent close to 2.5, and by Mallamace et al. [20] who observed a strong increase of the static shear viscosity in the vicinity of the percolation locus. On these basis, one would expect to observe a strong increase of the sound absorption both near the critical point (let us remind that in fluid systems made of particles having attractive potential, the percolation point is located near the critical point [32]. This is indeed the case for the AOT-based microemulsion systems) and the percolation point for microemulsion systems of higher volume fractions.

3. Experimental set-up and procedure

The surfactant AOT is purchased from Fluka Chem. Corp. and used without further purification, *n*-decane is an Aldrich 99% gold label product. The water is ultra pure high conductivity (18 MΩ) from Millipore. Solutions are prepared by dissolving the proper amount of surfactant in decane and by adding water. In the case of Rayleigh–Brillouin experiments, the samples are kept in a cylindrical optical glass vessel of 2 cm of diameter and sealed under vacuum. For ultrasonic experiments, the samples are contained in a stainless steel container, whereas for time domain reflectometry, the microemulsions are contained in Hewlett-Packard coaxial air guides whose walls are

coated by gold. Since it is known that AOT might undergo hydrolysis, the experiments are conducted rapidly on fresh samples. In all the cases, the sample housing was very carefully temperature controlled, typically ± 2 mK for periods of hours. The temperature of the sample is measured by a calibrated platinum resistor connected to a precision Whetstone bridge.

In microemulsions, most of the light is scattered in the non-shifted Rayleigh component arising from large concentration fluctuations, since it is usually difficult to achieve an excellent index matching between the droplets and the continuous phase. The intensity ratio between the central Rayleigh line and the two shifted Brillouin lines is typically in the range between 100 and 1000. So precise measurements of the frequency shift and line width of the Brillouin lines in these systems are a difficult task. Therefore, initially one has to choose a system in which a reasonable index matching is achieved between the water droplets and the continuous phase in order to minimise the influence of the concentration fluctuations. This is roughly the case of the system AOT-water-decane at a Water/AOT molar ratio $X = 40.8$. Also, the experimental set-up has to be optimised by using a multipass Fabry–Pérot interferometer with a well defined apparatus function. Such limitations occur neither in ultrasonic measurements nor in dielectric measurements.

The Brillouin spectrometer is depicted in Fig. 1. The light issued from the single frequency Spectra Physics Ar^+ laser is split into two beams. The first one with very low intensity is used for the alignment of the optical system and the control of the laser frequency. The second one whose intensity can be varied, is focused on the sample contained in a thermalised housing. A set of mirrors allows us to change the scattering angle θ and in turn the wave vector q. The scattered light is analysed by a multi-pass plane Fabry–Pérot interferometer having a typical finesse of the order 50. The fringe pattern is focused on a pinhole and the dispersed light is received by an avalanche photo diode having very high quantum efficiency and very low dark counts. After a convenient amplification and discrimination, the signal pulses feed a 1024 channels multichannel analyser (MCA). By using two rotating discs, we can record both the instrumental function and the Rayleigh–Brillouin spectrum sequentially on the MCA. They are, respectively, recorded on the first 200 channels of the analyser and on the last 824 channels. The duration of a scan of the MCA is 1 s and the typical duration of an experiment is 1000 s. In order to maximise the thermal and the mechanical stability of the set-up, the laser and all optical devices remain on a TMC anti-vibrating table and the room is temperature controlled with a precision of the order $\pm 1 \times 10^{-1}$ K. The whole set-up is driven by a PC computer via a National MCS hardware and software.

One has to keep in mind that in a Brillouin scattering experiment, the result of the measurement is not the dynamic structure factor $S(q, \omega)$ but its convolution by the instrumental function. In our case, the instrumental function is accurately known for each experiment, and can be accurately fitted to an Airy function. Therefore, we can then use Zamir et al.'s [33] analytical convolution procedure adapted to the case of a multi-pass instrument, to obtain both Ω_B and Γ_B. From these quantities we can derive
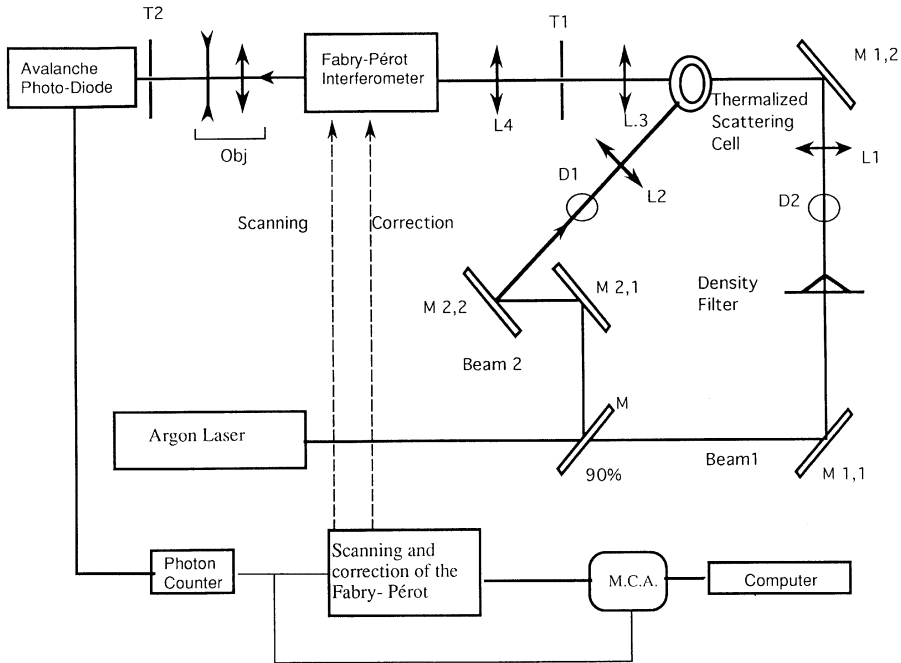
Fig. 1. Schematic view of the Brillouin spectrometer.

the hypersonic velocity and absorption with an accuracy, respectively, equal to $\pm 2\%$ and $\pm 10\%$. Let us emphasise here that the non-shifted line appears to have the same width as the instrumental function for the critical and off-critical microemulsions. This is connected to the fact that even for non-critical samples the slow concentration fluctuations are the dominant phenomenon. Concentration fluctuations in these systems have been measured by different authors [3–8]. Even far from T_C, the line width is in the kHz range due to the mesoscopic size of the microemulsion droplets, typically 80 Å and can be measured only by photon correlation spectroscopy. On the other hand, the entropy line is very weak compared to the concentration line (typically 1%). Although its width is comparable to that of the instrumental function and so in principle could be measured, it appears as noise on the concentration line and no information can be obtained.

Ultrasonic velocity and absorption have been measured on the same samples in the frequency range from 5 to 200 MHz by using a high precision MATEC ultrasonic spectrometer. In this case, the measurements directly give the sound velocity which is known for an accuracy better than 0.1%, whereas the accuracy for sound absorption is typically 10%. In order to deduce the so-called classical sound absorption, we have measured the static shear viscosity, and our data [12,13] are in agreement with those of Mallamace et al. [11,20] and Berg et al. [21].

The electrical conductivity and permittivity of the different samples have also been measured at low frequency from few Hz up to 13 MHz by using a Hewlett-Packard (HP) 4192 Low Frequency Impedance Analyser. Electrical data obtained at a higher frequency have been obtained both using a HP 4191A Radio Frequency Impedance Analyser for frequencies ranging from 1 MHz to 1 GHz and a time domain reflectometer up to 10 GHz. This last method is described in details by Cole et al. [15]. Repetitive fast rising voltage pulses (typical rising time 10 ps) generated by a pulse generator are sent through a sampling head (HP 54121A) on the sample contained in a H. P. coaxial air guide via a 50 Ω coaxial line. The signal reflected at the interface between the sample and the coaxial line, is analysed by the sampling head and stored in a fast sampling oscilloscope (HP 54120B) connected to a computer. A deconvolution procedure [15] has to be used then in order to deduce the frequency (or time) dependent dielectric properties of the microemulsion. In this type of experiments performed close to the critical temperatures, one has to take into account of heterogeneities which might appear in the mixture, leading to Maxwell–Wagner effect [36].

4. Experimental results and discussion

4.1. Critical microemulsion

A typical Rayleigh–Brillouin spectrum obtained for the microemulsion at the critical 10% composition, is depicted in Fig. 2. The sharp line on the left of the plot is the instrumental function centred on channel 100 of the MCA. The two Brillouin lines centred around channels 300 and 500 and the Rayleigh line centred around channel
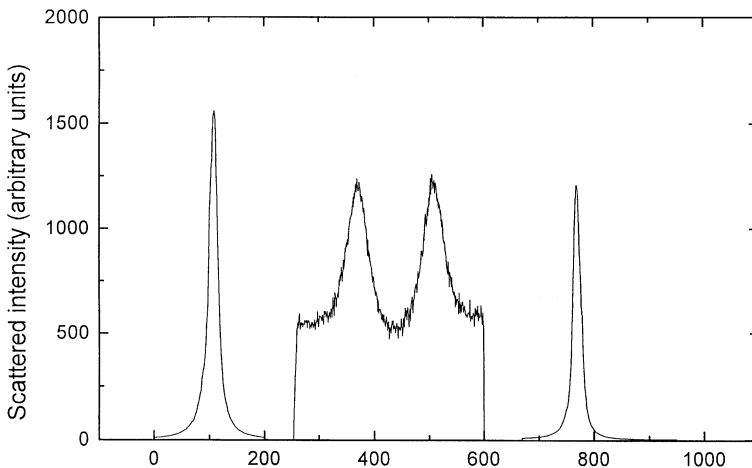
Fig. 2. Rayleigh–Brillouin spectrum of a critical AOT-water-decane microemulsion. Note that the amplitude of the Brillouin lines has been multiplied by 100.
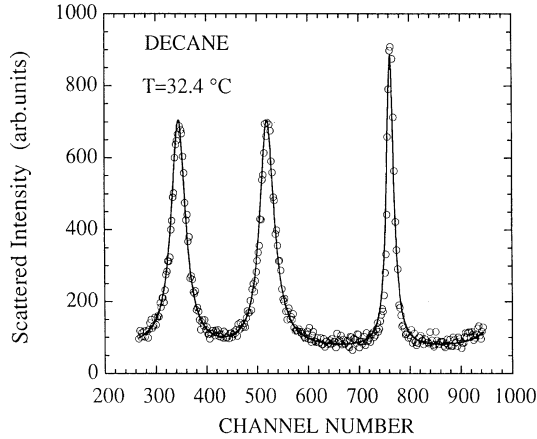
Fig. 3. Rayleigh–Brillouin spectrum of the decane continuous phase.

750, can be seen in the same figure. It has to be stressed that in order to be seen, the amplitude of the Brillouin lines was multiplied by 100. In this experiment, the central line has very nearly the same width as the instrumental function. The explanation of this effect is given above. Fig. 3 corresponds to the Rayleigh–Brillouin spectrum of the decane continuous phase. In this case, the experiment is easy since the amplitude of Brillouin lines is similar to that of the Rayleigh line.

Different quantities are accurately known for the AOT-water-decane microemulsion. In a previous study, we have reported on the relaxation rate of the concentration fluctuations inferred from light beating spectroscopy experiments [3–8]. We have shown that not only from very close critical point, but also in a rather large volume fraction domain, the system can be rather well described by mode-coupling theory including background when using a short range correlation length $\xi_0 = (13.3 \pm 1.5)$ Å and static values of the shear viscosity η_s, as reported by Berg et al. [21]. The refractive index and its very weak anomaly (the anamalous change in the index is about 6×10^{-3} for a temperature change of $14°C$) have also been very accurately measured by Pépin et al. [34,35]. On the other hand, we have very little information on the exact behaviour of the other transport or thermodynamic coefficients. Therefore, we will assume the dynamic structure factor $S(q, \omega)$ next, which is constituted of two unshifted Lorentzian lines (Rayleigh line) and two shifted Brillouin lines, where each line has been made of a Lorentzian and an anti-Lorentzian, as given by Berne and Pecora [16] for non-relaxing binary mixtures. A typical fit of the Brillouin doublet obtained by combining Berne and Pecora expression for $S(q, \omega)$ [16] and Zamir et al. [33] convolution procedure, is shown in Fig. 4. From the fit we can deduce the frequency shift Ω_B and the line width Γ_B. Using the formulas given in Section 2, we can extract both the hyper sound velocity and the sound absorption coefficient α/f^2 and compare these values to those inferred from low and high frequencies ultrasonic measurements.
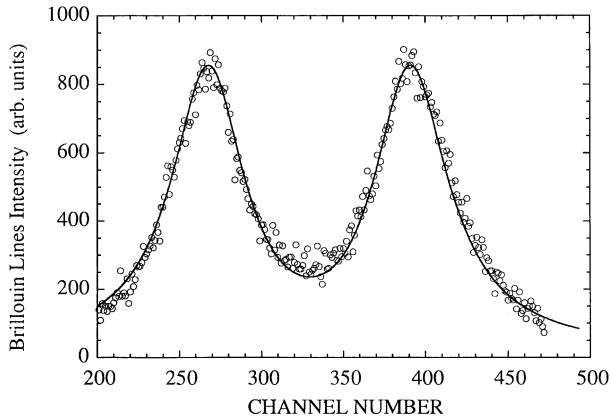
Fig. 4. Brillouin doublet of a critical AOT-water-decane microemulsion. The symbols are experimental data, whereas the full line is the best fit combining the dynamic structure factor $S(q, \omega)$ given by Berne and Pecora [16] and Zamir et al. [33] deconvolution procedure.
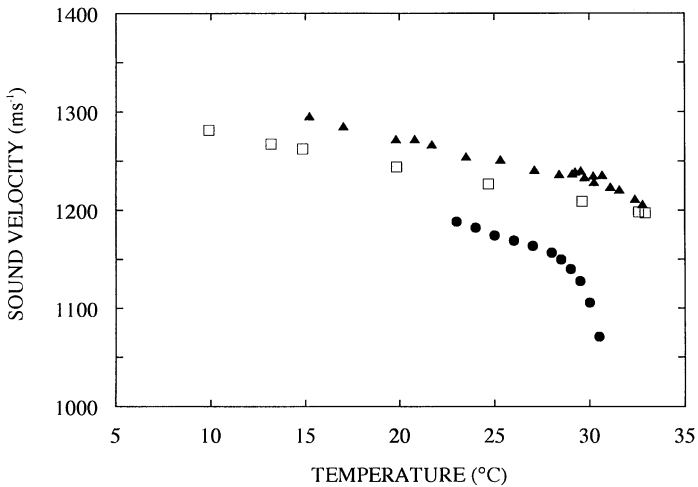

Fig. 5. Temperature variation of the sound velocity for a critical microemulsion. The triangles are hypersonic 5 GHz data, the squares are ultrasonic data at 25 MHz, the circles are 910 Hz, very low frequency ultrasonic data of Harada et al. [14].

The temperature variations of the sound velocity for the critical 10% microemulsion are reported in Fig. 5, the critical point for this particular system being located close to 33°C. The triangles and the squares are, respectively, related to Brillouin measurements and ultrasonic data at 25 MHz. On the same graph, we have also reported Harada and Tabuchi [14] data obtained at 910 Hz, but on a very slightly different system at $X = 40$. The values of the Brillouin frequency that we obtain at 20°C are typically 5.35 GHz and the hyper sound velocity we deduced is 1275 ms^{-1}. On the other hand,

ultrasonic data taken at 25 MHz lead to a velocity of 1245 ms^{-1}. Brillouin scattering and ultrasonic experiments have been performed on the same system by Ye et al. [9,10]. No quantitative comparison can be performed between results given in Refs. [9,10] and our data, since the operating temperature is not given in Refs. [9,10]. However, since the sound velocity taken at frequencies larger than few MHz is not too sensitive to temperature, our results are more than qualitative in agreement. Indeed values given by Ye et al. are close to 1240 ms^{-1} (see Fig. 3 in Ref. [6]). In all cases we observed a decrease in the sound velocity on approaching the critical temperature, but this decrease is much less pronounced for experiments conducted at ultrahigh (5.3 GHz) or high (from 5 to 55 MHz) frequencies than for those performed at a low frequency (910 Hz). We also observed that the lower the frequency, the lower is the sound velocity, but no significant differences were obtained for our ultrasonic experiments at frequencies between 5 and 55 MHz. This result is also in agreement with Ye et al. reports [9,10].

For the AOT-water-decane critical microemulsion, we can calculate the prefactor ω_0 of the Debye relaxation frequency. Using $T_C = 313$ K, the static shear viscosity $\eta = 1.5$ cP, and $\xi_0 = 13.3$ Å, we get $\omega_0 \approx 2.5 \times 10^6$ s^{-1} leading to a Debye relaxation frequency ranging from 500 kHz away from the critical point to 100 kHz at $\tau = 10^{-3}$, i.e. located in between Harada's and our ultrasonic measurements. These data are also consistent with Ye et al. findings, who report a relaxation frequency lower than 1 MHz [9,10]. From these values we can conclude that our Brillouin and ultrasonic data taken in the high frequency regime, should not show any sound dispersion. On the other hand, Harada and Tabuchi [14] measurements which have been performed in the low frequency limit should present sound dispersion. Indeed a strong sound dispersion is observed in Harada and Tabuchi data [14] in agreement with Ferell and Bhattacharjee [27] theoretical predictions. Assuming that Harada and Tabuchi [14] sound velocity measurements have been taken in the low frequency limit and that our Brillouin scattering data correspond to the high frequency limit, we have plotted the sound velocity dispersion as a function of the reduced temperature in Fig. 6. The sound dispersion ranges from few % away from the critical point to 10% close to T_c. We can see from Fig. 6 in double log plot, that the dispersion can be very well fitted to a power law, the exponent we extracted from the fit being (-0.37 ± 0.05). The absolute value of this exponent is nearly equal to the one characterising the shape of coexistence curve, usually noted as β in the literature, $\beta = 0.33$ for a 3-D Ising system.

The sound absorption coefficient α/f^2 related to the critical microemulsion obtained from Brillouin experiments (squares) and from ultrasonic experiments (circles) has been plotted vs. temperature in Fig. 7. As far as we know, this coefficient is reported here for the first time at hypersonic frequencies. Away from T_c, the very high frequency sound absorption α/f^2 remains almost constant and close to 50×10^{-17} cm^{-1} s^2. On approaching T_C, we observe a strong decrease in α/f^2, the value of which is about 20×10^{-17} cm^{-1} s^2 in the immediate vicinity of the critical point. This result is in apparent contradiction with the theoretical results (Eqs. (4) and (6)) predicting a divergence of this coefficient at the critical point. Our experimental result can be explained in the following way: It is well known that in complex fluids the bulk and shear viscosities
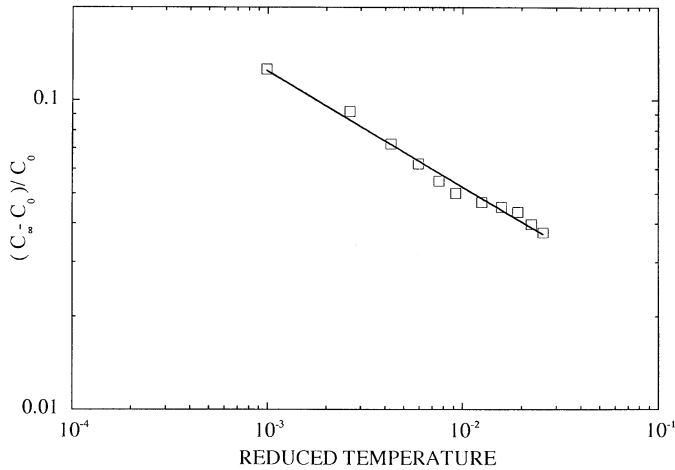
Fig. 6. Log–log plot of the sound dispersion vs. the reduced temperature. The squares are experimental data, the full line is the best fit of the experiment data to a power law.
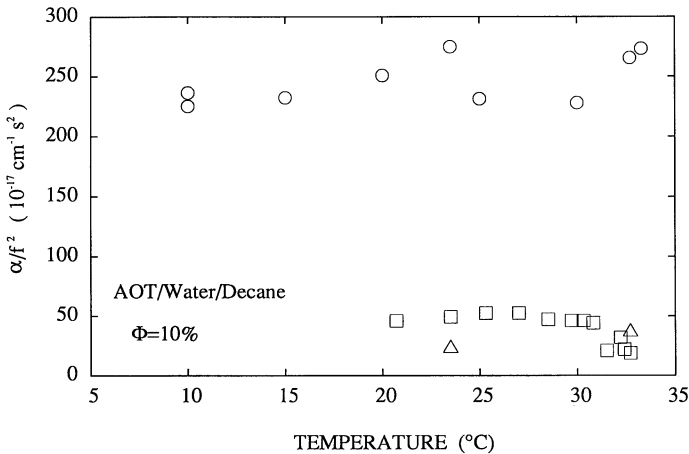

Fig. 7. The sound absorption coefficient of the critical microemulsion as a function of temperature. The circles are 25 MHz data, the squares are 5 GHz (Brillouin) data, the triangles are classical values calculated by taking into account only the static value of the shear viscosity.

show very strong frequency relaxations and are very weakly diverging near a critical point. Also not much is known about the amplitude of the barodiffusion coefficient and the values of the various thermodynamic coefficients appearing in the expression of the Brillouin line width. Our experimental results suggest that the main term governing the hyper sound absorption is the viscous term. The involved strongly diverging terms also have a small amplitude and should make a significant contribution to the absorption only in the immediate vicinity (few mK) from the critical point.
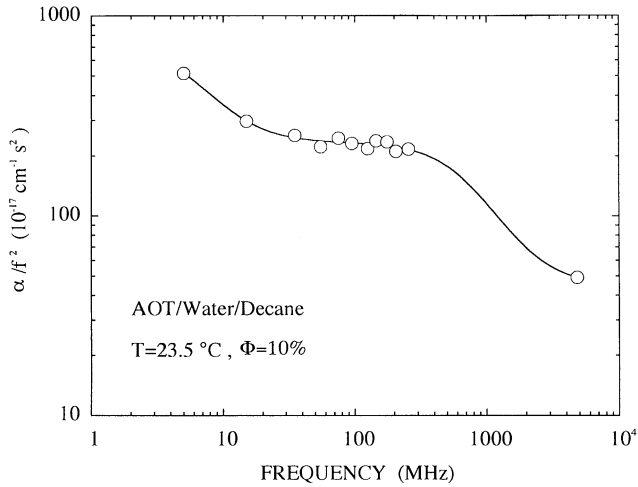
Fig. 8. Log–log plot of the sound absorption vs. frequency 10°C below T_C. The circles are experimental data, the full line is the best fit of the experimental data to a relaxation process given by Eq. (8), in the text.

To clarify this point, we have measured α/f^2 by ultrasound in a large domain of temperatures and frequencies. α/f^2 shows no singularity close to T_C and remains approximately a constant, and about 250×10^{-17} cm^{-1} s^2. Although it is difficult to compare this result with the findings of Zana et al. [12], we obtain very similar values for the absorption coefficient; however, the temperature dependence is quite different. In particular, we do not observe any significant increase of the sound absorption near the demixtion line. This might be due to some differences in volume fraction and molar ratio, respectively, equal to about 12% and 35 in Zana et al. experiments [12]. The experimental results however show that in the hydrodynamic regime the ultrasonic sound absorption coefficient is 6 times bigger than the hypersonic one, whereas in the critical regime, this ratio is about 12. We can compare these determinations of α/f^2 with the so-called classical absorption $(\alpha/f^2)_{\text{class}}$. In this case, only the static value of the shear viscosity is taken into consideration. As shown by Berg and Moldover [21], this quantity diverges at the critical point with an exponent nearly equal to 0.04. Therefore, in our domain of interest one should expect a significant increase of $(\alpha/f^2)_{\text{class}}$. This is again shown in Fig. 7. What is interesting to notice is that the hypersonic determination of α/f^2 close to T_C is smaller than the classical value, whereas the ultrasonic determination of α/f^2 in the same temperature range is much bigger. This result indicates a strong relaxation of the transport coefficients.

To gain precise information on the relaxation frequencies, we have measured the frequency dependence of α/f^2 in a large frequency range, from 5 MHz up to 5 GHz as a function of temperature. At a low temperature (Fig. 8), 10 K below T_C, we observe two well defined relaxation domains, one at low frequency, the other at high frequency. The frequency dependence of α/f^2 can be well accounted for by two Debye-like relaxation
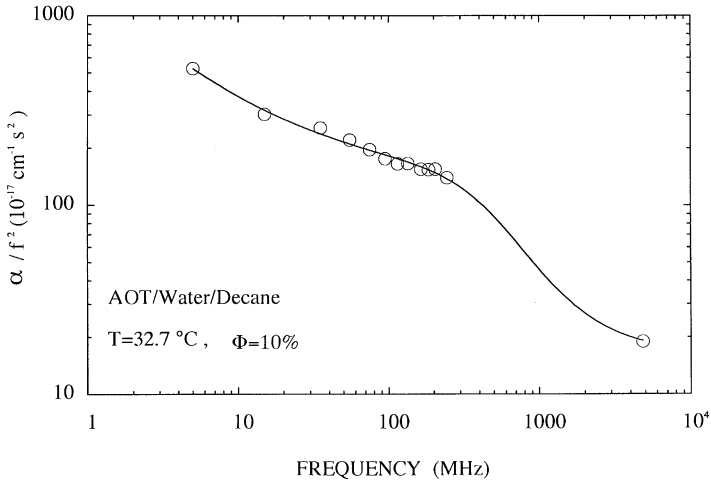
Fig. 9. Log–log plot of the sound absorption vs. frequency near T_C. The circles are experimental data, the full line is the best fit of the experimental data to a relaxation process given by Eq. (8), in the text.

processes:

$$\frac{\alpha}{f^2} = \left(\frac{\alpha}{f^2}\right)_\infty + \frac{A_1}{1 + (f/f_1)^2} + \frac{A_2}{1 + (f/f_2)^2},\qquad(8)$$

where the subscript ∞ indicates the infinite frequency value of the coefficient, in our case $(\alpha/f^2)_\infty = 44 \times 10^{-17}$ cm^{-1} s^2, A_i and f_i are, respectively, the amplitude and the relaxation frequency for the i-relaxation process. From the fit of our experimental result to Eq. (8) we obtain $A_1 = 480 \times 10^{-17}$ cm^{-1} s^2 and $f_1 = 6$ MHz for the low frequency relaxation domain and $A_2 = 190 \times 10^{-17}$ cm^{-1} s^2 and $f_2 = 800$ MHz for the high frequency relaxation domain, while the error on these parameters here is also of the order $\pm 10\%$. In Fig. 9, we have plotted the frequency variations of α/f^2 0.3 K below T_c. These data can be accurately be fitted to the same Eq. (8) and the values of the parameters we infer from the fit are: $(\alpha/f^2)_\infty = 20 \times 10^{-17}$ cm^{-1} s^2, $A_1 = 430 \times 10^{-17}$ cm^{-1} s^2 and $f_1 = 9$ MHz on one hand, and $A_2 = 190 \times 10^{-17}$ cm^{-1} s^{-1} and $f_2 = 260$ MHz on the other. The estimated uncertainties on these parameters are the same as above. On the other hand, a fit of the sound absorption coefficient to a power law in frequency as predicted by Kawasaki's theory, leads to a very large standard deviation. These results show that the low frequency relaxation domain is almost unaffected by the vicinity of the critical or percolation point. So, in disagreement with Zana et al. [12], we do not believe that the low frequency absorption is linked to percolation. Indeed, if we assume that close to the percolation threshold the systems are viewed as being made of transient fractal clusters, then the time of life τ_L of the cluster is close to the time it takes for a droplet to diffuse on a length scale corresponding to its radius R_H: $\tau_L = 6\pi\eta_s R_H^3/k_B T$. With the numerical values pertinent for the AOT microemulsion, the corresponding relaxation frequency would be close to 7×10^4 Hz, i.e., two orders of

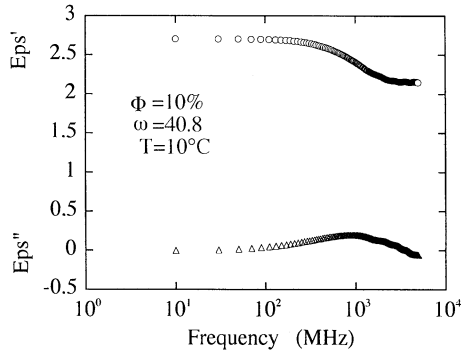Fig. 10. Plot of the real and imaginary parts of the dielectric constant as a function of frequency 23°C below the critical temperature. One can see that at low frequency the value 2.7 of the real part Eps$'$ is only slightly larger than the square of the refractive index n of the mixture ($n^2 = 2$); on the other hand, the maximum value of the imaginary part Eps$''$ is small, of the order of 0.3 at 1 GHz.

magnitude lower than the experimental result. We therefore believe that this relaxation phenomenon is probably connected to an intrinsic property of the microemulsion systems. Not only can a translational motion of the droplet be coupled to the sound wave but also shape fluctuations. Two processes can be considered. If the bending energy governs the fluctuations of the AOT film, the characteristic relaxation time τ_B is given by (see for instance the review articles by Auvray and Safran [36]): $\tau_B \approx \eta_s R_H^3 / K_R$, where K_R the rigidity coefficient of the film is of the order of $5k_B T$ [36]. With these numerical values, τ_B is of the order 24 ns and the corresponding frequency near 7 MHz, which is very similar to the experimental result. If the surface tension g of the film governs the fluctuations, the relaxation time τ_s is approximately given by: $\tau_s \approx \eta_s R_H / g$. The surface tension $g = 0.07$ dyn/cm of the AOT film has been measured by Farago et al. [37]. Although water and decane have been substituted, respectively, by heavy water and deuterated decane, we believe that this value of g can be used to evaluate $\tau_s \approx 100$ ns in the case of our system. The relaxation frequency we infer from this result is of the order of 1.5 MHz, i.e., of the same order of magnitude as the experimental result. So both fluctuations can contribute to the 6 MHz relaxation domain. On the other hand, the characteristic frequency of the high frequency relaxation domain is strongly lowered on approaching the critical point and denotes the critical slowing down or of percolation.

In order to complete these results, we have accurately measured the frequency-dependent dielectric properties of the critical sample in a large frequency domain. Typical result for the frequency dependent real part (Eps$'$) and imaginary part (Eps$''$) of the dielectric constant is plotted in Fig. 10 in a very broad frequency range. At a high volume fraction the relaxation of the droplet dipole moment is rather complex as shown by Feldman and coworkers [38–40]. Few studies have been reported at low volume fraction corresponding to the critical sample. In Fig. 11, we have plotted the real part (Eps$'$) of the dielectric permittivity as a function of frequency for the
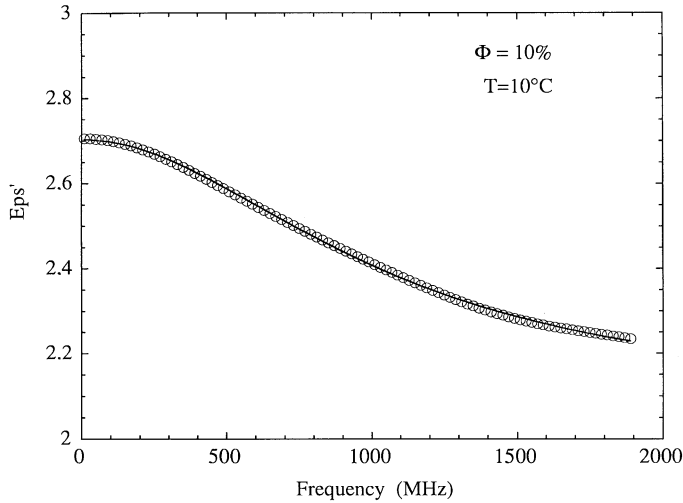
Fig. 11. Plot of the real part of the dielectric constant as a function of frequency at 10°C. The circles are experimental data, whereas the full line is the best fit to a single Debye relaxation process.
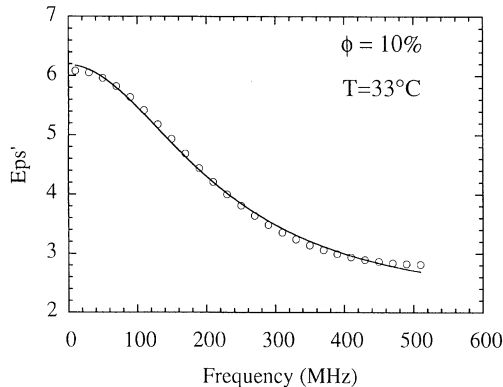

Fig. 12. Plot of the real part of the dielectric constant as a function of frequency very close to T_C. The circles are experimental data, whereas the full line is the best fit to a single Debye relaxation process.

critical microemulsion 23°C below T_c. These data can be accurately fitted to a single Debye relaxation process. From the fit, we can infer the relaxation frequency to be (800 ± 50) MHz. Very close to T_c (Fig. 12) we obtain a different result, i.e., the fit is not as good as the above and the relaxation process which occurs at much lower frequency (200 MHz) is of the Cole–Davidson type. This relaxation involves a distribution of relaxation time, or equivalently, the time-dependent dipole moment correlation function is a stretched exponential, a typical indication of the slow dynamic. Fitting our data to a Cole–Davidson relaxation process leads to a stretched exponent β close to 0.80 ± 0.05. This result is consistent with Feldman et al. [38–40] findings
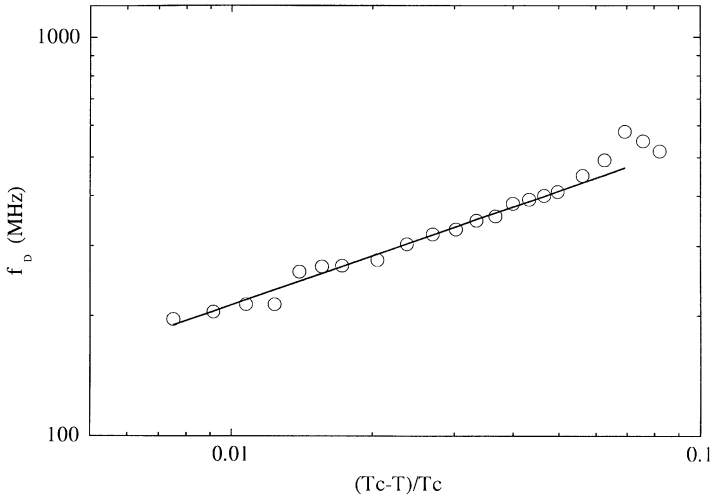
Fig. 13. Log–log plot of the dielectric Debye relaxation frequency as a function of the reduced temperature. The dots are experimental results, the full line is the best fit to a power law.

and corresponds to the clustering of the microemulsion droplets forming a transient fractal network [3–7,35]. A similar behaviour has been observed by Rouch et al. [41] for the concentration fluctuations correlation function which evolves continuously from a single exponential far from T_c to a stretched exponential close to T_c.

Since the departure from a single Debye relaxation process is rather weak, we can assume that it is at least not very close from the critical point, the relaxation of the dipole moment correlation function is of Debye type, so it is characterised by a single relaxation frequency f_D. We have plotted in Fig. 13 the temperature variation of f_D along the critical isochore. It can be seen that f_D ranges typically from 800 MHz at low temperature to 200 MHz close to T_c. For complex liquids this characteristic frequency f_D is known to be close to the viscosities relaxation frequency. This is also the case for the critical microemulsion, and as expected the values of f_D are close to those characterising the fast relaxation process revealed by the sound absorption measurements. The double log plot of Fig. 13 shows that f_D obeys a power law as a function of the reduced temperature, the exponent being $(+0.39 \pm 0.05)$. The absolute value of this exponent is very similar to the one we derived for the divergence of the sound dispersion and is also very close to the exponent β. As far as we know, no theoretical model is able to explain our experimental result.

The analysis of the relaxation of the dipole moment of the droplet in terms of a single Debye relaxation also provides the low (static) and high (infinite) frequency dielectric permittivities. These two quantities are plotted as a function of the reduced temperature in Fig. 14. The static permittivity increases significantly on approaching T_C and its temperature behaviour can be well accounted for by a power law with an exponent (-0.37 ± 0.05). The divergence of the static permittivity at T_C seems to be
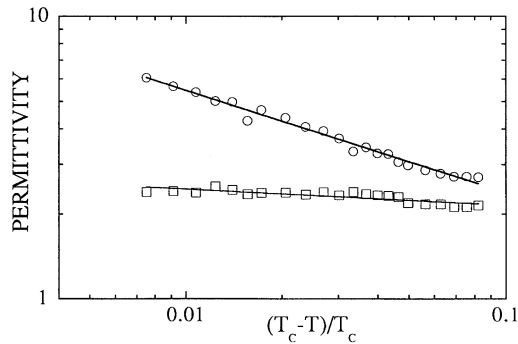
Fig. 14. Log–log plot of the static (circles) and infinite frequency (squares) dielectric constant as a function of the reduced temperature. The full lines are best fits to power laws.

in contradiction with Sengers et al.'s [30] theoretical predictions based on two scale universality. In this case, one would expect a finite value of the permittivity at the critical point. In fact, this unexpected behaviour can be understood if we realise that on the critical isochore the critical temperature is nearly the percolation point, where this quantity should diverge. It is interesting to note that the exponents characterising the divergences of the Debye relaxation frequency and of the static permittivity have almost the same absolute value, but of opposite signs. In Fig. 14 the temperature variations of the infinite frequency permittivity are also plotted. It seems to increase very slowly on approaching T_C and its variation can be fitted to a power law. In this case, however the exponent is very small (-0.06 ± 0.03), a value similar to the exponent characterising the divergence of the shear viscosity. Theoretical models are able to describe the behaviour of the low and infinite frequencies dielectric permittivities as a function of the distance from the critical point in volume fraction Φ. On approaching the percolation threshold and for both quantities, the theories predict a divergence described by the same exponent s of the order of $s = -1.2$ [3–7]. In the case of an approach in temperature, our experimental results show that the exponents are very different from those inferred from an approach in Φ, but are, respectively, similar to those describing the divergence of the sound velocity dispersion and of the shear viscosity. As far as we know, and in this case too, no theoretical model is able to explain these new experimental results.

4.2. Dense microemulsion

The electrical conductivities of dense microemulsions have been measured in detail by many authors [3–7], so they will not be discussed here. However, in order to locate the percolation threshold we have measured both the inflexion point of the low frequency electrical conductivity and the maximum of the low frequency electrical permittivity as a function of temperature. We obtained, respectively, $20°C$ for the $\Phi = 50\%$ sample and $10°C$ for the $\Phi = 75\%$ sample.
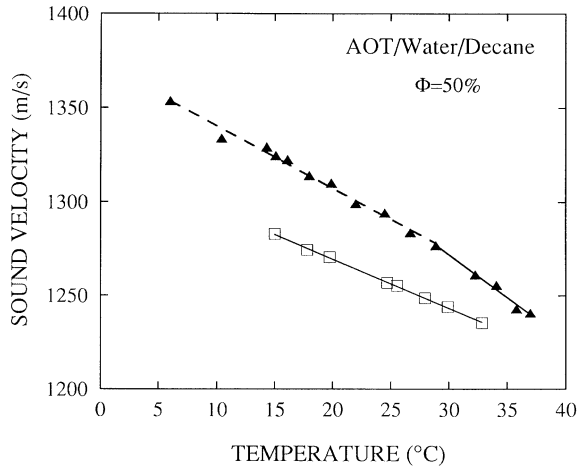
Fig. 15. Sound velocity as a function of temperature for a 50% AOT-water-decane. The circles are data obtained from Brillouin scattering, whereas the squares are ultrasonic data at 25 MHz data.
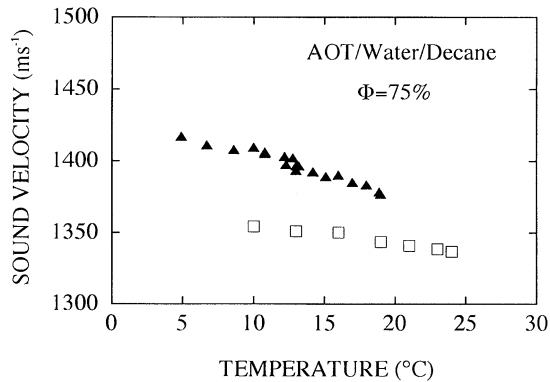

Fig. 16. Sound velocity as a function of temperature for a 75% AOT-water-decane. The circles are data obtained from Brillouin scattering, whereas the squares are ultrasonic data at 25 MHz data. Note that at this composition the microemulsion is probably in the L_3 (spongeous) phase.

Measurements of the Brillouin doublet is rather difficult at these concentrations since the amplitude of the Brillouin lines is very weak. Figs. 15 and 16 show the typical temperature variations of the hypersonic and ultrasonic sound velocity for microemulsions, respectively, at $\Phi = 50\%$ and $\Phi = 75\%$ volume fraction. The triangles are the Brillouin data and the squares represent the ultrasonic 20 MHz results. In the case of the $\Phi = 50\%$ microemulsion, we observe that the hypersonic sound velocity decreases upon increasing temperature from typically 1350 to 1250 ms^{-1}, whereas the ultrasonic velocity decreases from 1290 ms^{-1} at 10°C to 1250 ms^{-1} at 32°C. So the sound dispersion decreases from about 40 ms^{-1} at 10°C to 20 ms^{-1} at 32°C. These results are in overall agreement with Ye et al. [10] findings, although the size of the microemulsion
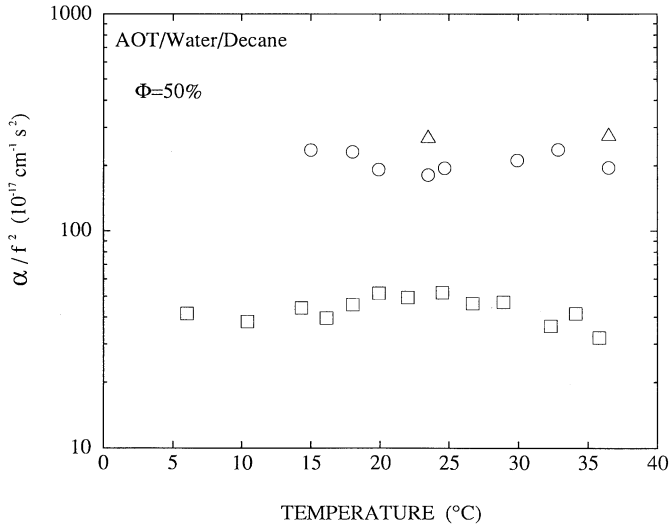
Fig. 17. The absorption coefficient as a function of temperature for a 50% AOT-water-decane. The circles are 25 MHz data, the squares are 5 GHz (Brillouin) data and the triangles are classical absorption values.

droplet at the same volume fraction is different in Ye et al. report (see Fig. 5 of Ref. [10]). In the case of the more dense microemulsion, the hypersonic velocity ranges from 1420 to 1370 ms^{-1} when the temperature increase from 2°C to 18°C and the sound dispersion varies from typically 50 to 20 ms^{-1} in the same temperature range. When crossing the percolation threshold for the two samples, we do not observe any strong anomaly on the speed of the sound. However, a small but significant change on the slope of the velocity vs. temperature curve for the 75% microemulsion is observed at the percolation threshold. Although no direct comparison can be made, these results are in overall agreement with Ye et al. findings [10]; these authors report a sound velocity increasing with the volume fraction and a dispersion typically of the order 50 ms^{-1} (see Fig. 5 of Ref. [10]).

For the same systems, the absorption coefficient α/f^2 is plotted as a function of temperature in Figs. 17 and 18. For the 50% sample (Fig. 17), the hypersonic absorption measured for the first time, shows a broad maximum close to 50×10^{-17} cm^{-1} s^2 around the electrical conductivity percolation threshold located at 20°C. On the other hand, this maximum is not observed in the ultrasonic determination of α/f^2 taken at 25 MHz. In this case, α/f^2 remains almost constant and close to (220 ± 20) 10^{-17} cm^{-1} s^2, a value about 5 times larger than the hypersonic determination. We observed the same situation for the 75% microemulsion (Fig. 18) in this case, whereas the ultrasonic absorption is almost constant in the whole temperature domain we studied and close to 270×10^{17} cm^{-1} s^2; the hypersonic absorption is more peaked at the percolation threshold and is equal to 80×10^{-17} cm^{-1} s^2. These values can be compared to the classical absorption coefficient, only due to the shear viscosity. From the data of the
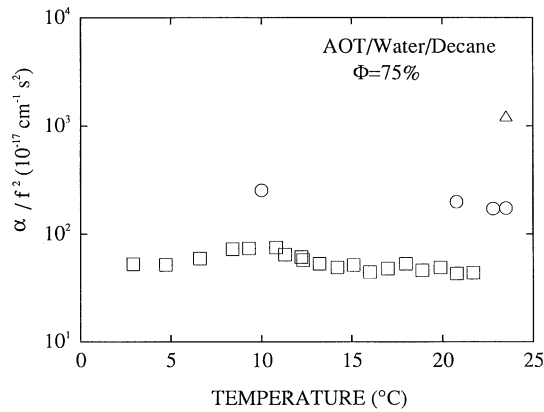
Fig. 18. The absorption coefficient as a function of temperature for a 75% AOT-water-decane microemulsion. The labels are the same as for Fig. 17. Note however that the ordinate is in a log scale.
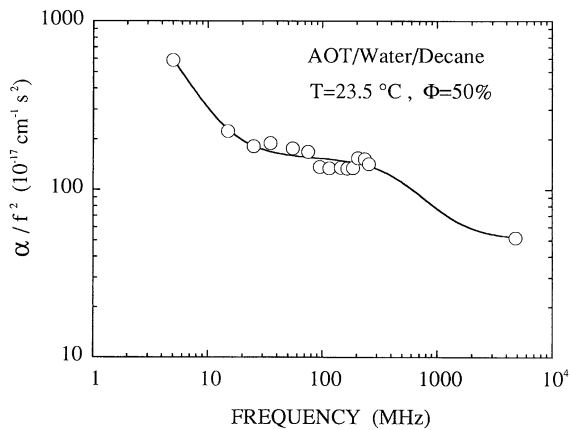

Fig. 19. The absorption coefficient as a function of frequency for a 50% AOT-water-decane microemulsion at $t = 23.5$°C. The circles are experimental results, whereas the full line is the best fit to the data of a relaxation process having two different characteristic times according to Eq. (8), in the text.

shear viscosity reported by Mallamace et al. [11,20] and Cametti et al. [13] one infers classical values of the absorption coefficient, close to 270×10^{-17} cm^{-1} s^2 for the 50% sample, i.e., slightly larger than the ultrasonic value, and 1200×10^{-17} cm^{-1} s^2 for the 75% microemulsion, i.e., much larger than the ones given above for the same system. These effects are connected to a strong relaxation of not only the bulk viscosity but also of the shear viscosity and are typical of the viscoelastic behaviour previously observed by ultrasonic techniques on dense micromulsions [10–13].

In order to deduce the relaxation frequencies, we have measured the frequency dependence of α/f^2 for the two samples at different temperatures (Figs. 19–21). For both systems, the absorption shows two well defined relaxation domains, respectively,
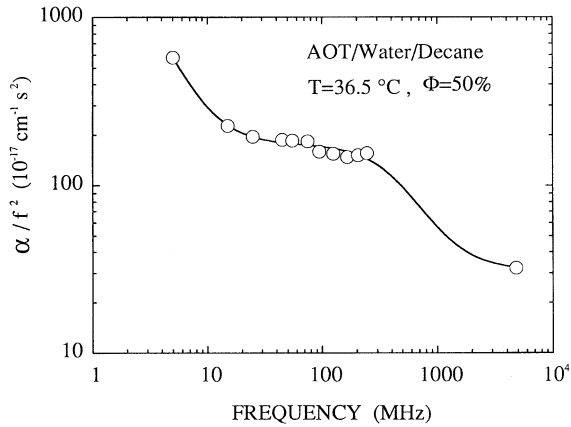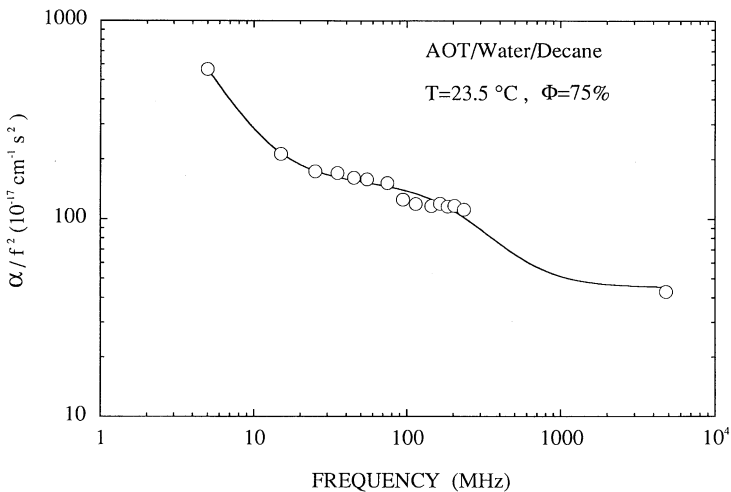
Fig. 20. Same caption as Fig. 19, but $t = 36.5°$C.

Fig. 21. Same caption as Fig. 19, but $\Phi = 75\%$.

located at low and high frequencies. From the fit of the experimental data to Eq. (8) we can derive the amplitudes and the characteristic frequencies of the two relaxation processes. For the two microemulsions, the most important relaxation process (90% of the total amplitude of the relaxation) is located at a low frequency. The corresponding relaxation frequency, of the order of 5 ± 2 MHz, is almost independent of temperature and volume fraction. It has to be stressed that this value is nearly equal to the one describing the low volume fraction critical sample. This reinforces our hypothesis of linking this low frequency value to the intrinsic property of the AOT based microemulsion system. On the other hand, the high frequency relaxation domain is both temperature and volume fraction dependent. In particular, its characteristic frequency

decreases upon an increasing Φ. As an example, at $23.5°C$ the frequencies are, respectively, equal to $600\,MHz$ at 50% and $250\,MHz$ at 75%. It has to be noted, however, that for the 75% microemulsion, $23.5°C$ probably corresponds to a randomly oriented lamellar phase.

It has been shown by Ye et al. [10] and by Cametti et al. [13] that the frequency dependence of ultrasonic data taken at high volume fraction can be explained in terms of the theory of the viscoelasticity [42]. The relaxation of the two viscosities (shear and bulk) is described by a Cole–Davidson relaxation processes. The relaxation times deduced by Cametti et al. [12,13] were, respectively, $23.2\,ns$ at $\Phi = 50\%$ and $122\,ns$ at $\Phi = 75\%$. These values correspond to relaxation frequencies in the MHz domain and are in agreement with the relaxation frequencies we deduced for the low frequency relaxation domain. To be consistent with our experimental results taken in a very broad frequency range and showing two well defined relaxation domains having very different relaxation times, we are tempted to express phenomenologically the shear and the bulk viscosity in the following way:

$$\eta_s(\omega, \Phi, T) = \frac{G_\infty^1 \tau_s^1}{1 + (\omega \tau_s^1)^2} + \frac{G_\infty^2 \tau_s^2}{1 + (\omega \tau_s^2)^2} \,,$$

$$\eta_B(\omega, \Phi, T) = \frac{K_r^1 \tau_B^1}{1 + (\omega \tau_B^1)^2} + \frac{K_r^2 \tau_B^2}{1 + (\omega \tau_B^2)^2} \,, \tag{9}$$

where G_∞ denotes the infinite frequency shear modulus, K_r the relaxational part of the compressional modulus, $K_r = K_\infty - K_0$, where K_∞ and K_0 are, respectively, the infinite frequency and static compressional modulus. The relaxation times τ_s and τ_B are, respectively, connected to the relaxing shear and bulk viscosities; the labels 1 and 2 denote, respectively, the low and high frequency relaxation processes. At zero frequency, one obtains, respectively, $\eta_s = G_\infty^1 \tau_s^1 + G_\infty^2 \tau_s^2$ and $\eta_B = K_r^1 \tau_B^1 + K_r^2 \tau_B^2$. As a first approximation, we can assume that the relaxation times of the shear and bulk viscosities are similar which is a typical result for viscous liquids like glycerol, and that the numerical values obtained for G_∞ and K_r by Cametti et al. [13] are those relevant for the slow relaxation process. In the case of the $\Phi = 50\%$ sample, one would obtain very small (even negative) values for the parts of the infinite frequency shear modulus and compressional modulus, characterising the fast process. In the case of the 75% sample, assuming $G_\infty^1 = 0.8 \times 10^7\,N\,m^{-2}$, $K_r^1 = 3 \times 10^8\,N\,m^{-2}$ and $\eta_s = 0.11\,Ps$ [12,13], we infer $G_\infty^2 = 1.2 \times 10^8\,N\,m^{-2}$, and $K_r^2 = 2.3 \times 10^9\,N\,m^{-2}$. So the moduli characterising the fast process seem to be about 10 times larger than those describing the slow one and are of the same order of magnitude of those extrapolated from Fig. 6 of Ye et al.'s paper [10].

For the same 75% microemulsion, the plot in Fig. 22 which shows the temperature variations of the sound absorption measured at $5\,GHz$ (squares) and of the static dielectric constant (circles) is very interesting. Both quantities show a strong increase on approaching the percolation threshold, and when the units are conveniently chosen they behave in a very similar way. On the other hand, the sound absorption deduced
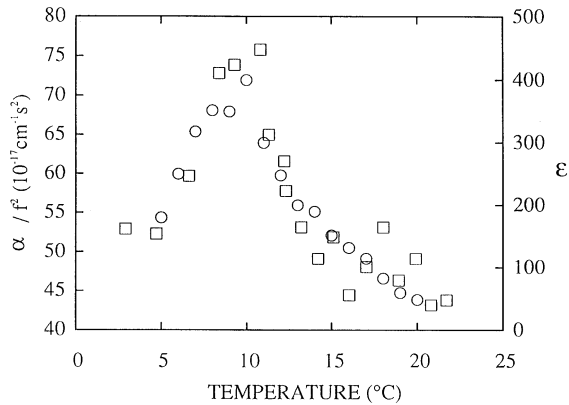
Fig. 22. Plot of the sound absorption coefficient (left scale) measured by Rayleigh–Brillouin spectroscopy and of the dielectric constant (right scale) as a function of temperature for a $\Phi = 75\%$ AOT-water-decane microemulsion. The maximum value of the coefficients around $t = 10^{\circ}$C corresponds to the electrical conductivity percolation threshold.

from ultrasonic measurements is nearly constant in the entire temperature range. No firm explanation can be given presently for these results.

5. Conclusion

In this paper, we have reported a very extensive set of new experimental data on AOT based water-in-oil microemulsion systems both in temperature and volume fraction. We have shown that combining different experimental techniques, namely very low frequency and high frequency ultrasonic measurements, very high frequency Brillouin scattering experiments and low and high frequency dielectric measurements, provide very interesting new results on the relaxation phenomena in these systems. In particular, we observed two relaxation regimes in a critical AOT-water-decane microemulsion system at a molar ratio of 40.8. The characteristic frequency of the low frequency relaxation process is located in the MHz domain, whereas the fast relaxation occurs at much higher frequencies, between 1 and 0.1 GHz. The characteristic frequency of the slow process, typically 5 MHz, is almost independent of temperature. So it is not connected to the critical slowing down or to percolation and it is probably an intrinsic characteristic of the AOT microemulsion. The fast process has a correlation time nearly equal to the dielectric relaxation time in the large temperature domain we studied and shows the typical critical slowing down effect. This fast relaxation process observed for the first time by Brillouin scattering, might be linked to structural arrangements of a transient quasi-solid fractal network arising from long range attractive interactions among droplets, as speculated by Ye et al. [9,10]. To account for the critical sound velocity dispersion in the vicinity of the critical temperature, another relaxation process should exist at very low frequency, typically in the kHz range, corresponding to the

Debye–Kawasaki relaxation frequency, and connected to the time of life of the transient fractal cluster. As far as we know, this process has not yet been observed by ultrasound technique. We also show for the first time that the sound dispersion, the Debye high frequency dielectric relaxation time and the static dielectric constant are singular at the critical point (or equivalently, the percolation point) with nearly the same absolute values of the critical exponent, close to that of the index $\beta = 0.33$ characterising the shape of the coexistence curve in the vicinity of T_C. The divergences of the dielectric constant and of the Debye relaxation time at the critical point can be explained by the fact that in the AOT based microemulsion, the critical consolute point is nearly identical to the percolation point like systems with attractive potential. However, the values of the exponents we derived from the fits of sound dispersion, relaxation frequency, dielectric constants, etc., to the reduced temperature cannot be presently explained theoretically.

Dense microemulsions also show new interesting relaxation effects. For instance, for the dense $\Phi = 75\%$ microemulsion, we measured for the first time as far as we know, a very high frequency sound absorption coefficient which is about 30 times smaller than the classical absorption coefficient. From these very careful Brillouin scattering measurements and combining them with our ultrasonic data, we have also observed here a new fast relaxation process which accounts for typically 10% of the total absorption. Assuming the relaxation times for the shear and bulk viscosities to be the same, we have been able to approximately calculated the infinite frequency shear modulus and the relaxing bulk modulus connected to this fast process. Furthermore, we have also shown that for the microemulsion at $\Phi = 75\%$, the static electrical permittivity and the hypersonic frequency sound absorption coefficient behave in a completely similar way when crossing the percolation threshold in temperature, where they show a well defined maximum. This maximum is much more peaked than the one, very broad, observed by Mallamace et al. [20] for the shear viscosity of the microemulsion at the same volume fraction. At high volume fraction, the microemulsion could be viewed as being formed by a transient solid-like network characterised by a quite well defined elastic moduli and arising from the attractive interactions among droplets, in agreement with the idea proposed by Ye et al. [9,10], Zana et al. [12] and Cazabat et al. [32]. However, this solid-like network is very fragile since the values we obtain for the moduli are about 100 smaller than the ones obtained for glass forming liquids (typically of the order of 10^9–10^{10} Nm^{-2}). Now by comparing the data obtained at low volume fraction and high volume fraction, it can be seen that the frequency of the slow relaxation process, typically 5 MHz, remains unchanged when varying temperature and volume fraction, i.e., when approaching the percolation threshold both in temperature and concentration. We therefore believe that this slow process is likely to connect to an intrinsic property of the system as for the critical sample, and is not on indicator of percolation. From a numerical estimate of the relaxation frequencies of different plausible processes, membrane fluctuations governed either by the binding energy or by the surface tension could be responsible for this 5 MHz relaxation domain. However, the correlation times of these two processes scale in a different way as compared to the hydrodynamic radius

of the water droplet, respectively, like R_H^3 and R_H. As shown by Farago et al. [37], SANS and neutron spin echo measurements are more likely in favour of the influence of the binding energy since the relaxation time deduced from their experiments scales like R_H^3. As a final comment, in order to obtain more theoretical details on the dynamics of dense microemulsion systems and to explain for instance the scaling behaviours, we observed that for some physical parameter characterising the critical system, it would be interesting to extend Sorensen et al. droplet model [43] which has been shown to be valid for dilute critical systems.

Acknowledgements

References

[1] See for instance K.L. Mittal (Ed.), Micellization, Solubilisation, and Microemulsions, Plenum Press, New York, 1977.
[2] P. Tartaglia, J. Rouch, S.H. Chen, Phys. Rev. A 45 (1992) 7257.
[3] S. Bhattacharrya, J.P. Stokes, M.W. Kim, J.S. Huang, Phys. Rev. Lett. 55 (1985) 1884.
[4] J.A. van Dijk, Phys. Rev. Lett. 55 (1985) 1003.
[5] J. Peyrelasse, M. Moha-Ouchane, C. Boned, Phys. Rev. A 38 (1988) 4155.
[6] C. Cametti, P. Codastefano, P. Tartaglia, J. Rouch, S.H. Chen, Phys. Rev. Lett. 64 (1990) 1461.
[7] C. Cametti, F. Sciortino, P. Tartaglia, J. Rouch, S.H. Chen, Phys. Rev. Lett. 75 (1995) 569.
[8] J. Rouch, A. Safouane, P. Tataglia, S.H. Chen, J. Chem. Phys. 90 (1989) 3756.
[9] L. Ye, D.A. Weitz, Ping Sheng, S. Bhattacharya, J.S. Huang, M.J. Higgins, Phys. Rev. Lett. 63 (1989) 363.
[10] L. Ye, D.A. Weitz, Ping Sheng, J.S. Huang, Phys. Rev. A 44 (1991) 8249.
[11] F. Mallamace, N. Micali, C. Vassi, G. D'arrigo, Phys. Rev. A 43 (1991) 5170.
[12] R. Zana, J. Lang, O. Sorba, A.M. Cazabat, D. Langevin, J. Phys. Lett. 43 (1982) L–829.
[13] C. Cametti, P. Codastefano, G. D'Arrigo, P. Tartaglia, J. Rouch, S.H. Chen, Phys. Rev. A 42 (1990) 3421.
[14] Y. Harada, M. Tabuchi, Slow Dynamics in Condensed Matter, AIP Conferences Proceedings, 1992, pp. 320–321.
[15] R.H. Cole, J.G. Berberian, S. Mashimo, G. Chryssikos, A. Burns, E. Tombari, J. Appl. Phys. 62 (1989) 793 and references therein.
[16] B.J. Berne, R. Pecora, in: Dynamic Light Scattering, Wiley, New York, 1976.
[17] F.B. Hicks, T.C. Van Vechten, C. Franck, Phys. Rev. E 55 (1997) 4158.
[18] M. Giglio, A. Vendramini, Phys. Rev. Lett. 34 (1974) 561.
[19] M. Giglio, A. Vendramini, Phys. Rev. Lett. 38 (1976) 26.
[20] F. Mallamace, N. Micali, D. Lombardo, in: Structure and Dynamics of Strongly Interacting Colloids and Supramolecular Aggregates in Solution, Kluwer Acad. Pub., Dordrecht, 1992, pp. 405–417.
[21] R.F. Berg, M.R. Moldover, J.S. Huang, J. Chem. Phys. 87 (1987) 3687.
[22] J.P. Delville, C. Lalaude, S. Buil, A. Ducasse, Phys. Rev. E 59 (1999) 5804.
[23] K. Kawasaki, Phys. Rev. A 1 (1970) 1750.
[24] G. D'Arrigo, L. Mistura, P. Tartaglia, Phys. Rev. A 1 (1970) 286.
[25] G. D'Arrigo, L. Mistura, P. Tartaglia, Phys. Rev. A 3 (1971) 1718.

[26] L. Mistura, in: M.S. Grenn (Ed.), Proceedings of the Varenna Summer School on Critical Phenomena, Academic Press, New York, 1971.
[27] R.A. Ferrel, J.K. Bhattacharjee, Phys. Rev. A 31 (1985) 1788 and references therein.
[28] C.W. Garland, G. Sanchez, J. Chem. Phys. 76 (1983) 3090.
[29] C.W. Garland, G. Sanchez, J. Chem. Phys. 79 (1983) 3100.
[30] J.V. Sengers, D. Bedeaux, P. Mazur, S. Greer, Physica A 104 (1980) 573.
[31] P.G. de Gennes, J. Phys. (Paris) 37 (1976) L1.
[32] A.M. Cazabat, D. Chatenay, D. Langevin, J. Meunier, Faraday Discuss. Chem. Soc. 76 (1982) 291.
[33] E. Zamir, N.D. Gershon, A. Ben Reuven, J. Chem. Phys. 55 (1969) 3397.
[34] See for instance J. Hamelin, T.K. Bose, J. Thoen, Phys. Rev. E 53 (1996) 779.
[35] C. Pépin, T.K. Bose, J. Thoen, Phys. Rev. A 39 (1989) 835.
[36] L. Auvray, S.A. Safran, in: W.G. Gelbart, A. Ben-Shaul, D. Roux (Eds.), Micelles, Membranes, Microemulsions, and Monolayers, Springer, New York, 1994.
[37] B. Farago, D. Richter, J.S. Huang, S.A. Safran, S.T. Milner, Phys. Rev. Lett. 65 (1990) 3348.
[38] Y. Feldman, N. Kozlovich, I. Nir, N. Garti, Phys. Rev. E 51 (1995) 478.
[39] Y. Feldman, N. Kozlovich, I. Nir, N. Garti, Phys. Rev. E 54 (1996) 5420.
[40] N. Kozlovich, A. Puzenko, Y. Alexandrov, Y. Feldman, Colloids and Surf., to be published.
[41] J. Rouch, P. Tartaglia, S.H. Chen, Phys. Rev. Lett. 71 (1993) 1947.
[42] A.J. Matheson, Molecular Acoustics, Wiley, New York, 1971.
[43] C.M. Sorensen, R.C. Mockler, W.J. O'Sullivan, Phys. Lett. A 64 (1977) 301.